Remote Sensing of Environment 113 (2009) 1163–1174

Contents lists available at ScienceDirect

Remote Sensing of Environment

journal homepage: www.elsevier.com/locate/rse

Classifying species of individual trees by intensity and structure features derived from airborne laser scanner data

Hans Ole Ørka *, Erik Næsset, Ole Martin Bollandsås

Department of Ecology and Natural Resource Management, Norwegian University of Life Sciences, P.O. Box 5003, NO-1432 Ås, Norway

ARTICLE INFO

Article history:
Received 12 October 2007
Received in revised form 7 January 2009
Accepted 7 February 2009

Keywords:
Airborne laser scanning
Intensity
Species classification
Spruce
Birch

ABSTRACT

The objective of this study was to identify candidate features derived from airborne laser scanner (ALS) data suitable to discriminate between coniferous and deciduous tree species. Both features related to structure and intensity were considered. The study was conducted on 197 Norway spruce and 180 birch trees (leaves on conditions) in a boreal forest reserve in Norway. The ALS sensor used was capable of recording multiple echoes. The point density was 6.6 m^{-2}. Laser echoes located within the vertical projection of the tree crowns, which were assumed to be circular and defined according to field measurements, were attributed to three categories: "first echoes of many", "single echoes", or "last echoes of many echoes". They were denoted FIRST, SINGLE, and LAST, respectively. In tree species classification using ALS data features should be independent of tree heights. We found that many features were dependent on tree height and that this dependency influenced selection of candidate features. When we accounted for this dependency, it was revealed that FIRST and SINGLE echoes were located higher and LAST echoes lower in the birch crowns than in spruce crowns. The intensity features of the FIRST echoes differed more between species than corresponding features of the other echo categories. For the FIRST echoes the intensity values tended to be higher for birch than spruce. When using the various features for species classification, maximum overall classification accuracies of 77% and 73% were obtained for structural and intensity features, respectively. Combining candidate features related to structure and intensity resulted in an overall classification accuracy of 88%.

1. Introduction

In recent years, high resolution sampling density airborne laser scanning (ALS) has become readily available, providing *x*, *y*, *z* point datasets with 5–20 height measurements per square meter. Such data are useful for terrain, vegetation, and forest mapping. From these dense point clouds, individual trees can be identified by means of various segmentation procedures. These procedures extract the outline of the tree crowns. Individual tree segmentation is often done by using an ALS-derived canopy height model (e.g. Hyyppä et al., 2001; Persson et al., 2002; Solberg et al., 2006), but also other methods are used, like for example clustering (Morsdorf et al., 2004). When the outline of a tree crown is defined, laser echoes inside the segment can be tied to the tree and information about the tree such as stem position, height, and stem diameter can be derived (e.g. Persson et al., 2002; Solberg et al., 2006). This high resolution tree information can form a basis for forest planning by aggregating information to management units (Hyyppä et al., 2001).

Tree species is another parameter that may be derived from laser echoes inside individual tree segments. Species classification on a individual tree level using ALS-derived features has been accomplished in boreal forest in Scandinavia (Holmgren et al., 2008; Holmgren & Persson, 2004; Liang et al., 2007), in mixed coniferous and deciduous forest in central Europe (Heurich, 2006; Reitberger et al., 2008), in deciduous forest in western Virginia (Brandtberg, 2007; Brandtberg et al., 2003), and in sub-tropical forest in Queensland, Australia (Moffiet et al., 2005). Individual tree species information could also be found using high spatial resolution images (e.g. Brandtberg, 2002; Carleer & Wolff, 2004; Key et al., 2001; Olofsson et al., 2006). However, acquisition of both ALS data and imagery will increase inventory costs. Furthermore, because ALS provides more accurate estimates of biomass and height compared to image remote sensing methods (Hyde et al., 2006; Hyyppä & Hyyppä, 1999), the possibilities of utilize ALS data also to discriminate between tree species are of interest in order to control data acquisition cost.

Structural features of the tree crowns can be derived from ALS height measurements and such features might be considered for tree species classification. The basic idea behind using structural features for tree species classification is that different species have different crown properties such as crown shape, reflectivity, and location of biomass. For example, crown shapes for spruce trees tend to be conical, whereas more spherical or rounded shapes are found for deciduous trees. Deciduous trees also tend to allocate more biomass higher in the crown. The structural differences of tree crowns will

* Corresponding author. Tel.: +47 64965799; fax: +47 64965802.
E-mail address: hans-ole.orka@umb.no (H.O. Ørka).

0034-4257/$ – see front matter
doi:10.1016/j.rse.2009.02.002

influence on the recorded laser echoes. When a laser echo is recorded, the elapsed time between emission and receipt of a significant amount of returned energy is converted to range. Since the position and orientation of the platform are known by Global Navigation Satellite Systems (GNSS) and Inertial Navigation System (INS), the position of the target can be calculated. To trigger a laser echo from a tree crown or any other surface, the properties of the surface hit by the laser pulse is of importance. One example is the high rate of success in detecting power lines. A power line covers just a small portion of a laser footprint, but is still detectable in an ALS dataset because of the high reflectivity of power lines. On the other hand, a tree crown surface represented by branches and leaves often covering the entire laser footprint has lower reflectivity and a different structure. The laser pulse will therefore tend to penetrate into the canopy before a significant echo is recorded by the sensor (Gaveau & Hill, 2003). Thus, different crown properties affect the distribution of laser echoes within and on the surface of the tree crowns. This may lead to distinct echo height distributions for separate species. Therefore, it might be useful for automated species classification based on ALS data to identify which structural features derived from the echo height distribution that are most suited to distinguish species.

In addition to the spatial coordinates of laser echoes, most ALS systems measure the intensity of the backscattered laser signal (Wehr & Lohr, 1999). For pulse lasers, intensity often represents the peak amplitude of the returned pulse. It is expected that this value could assist species classification. Already in 1985, Schreier et al. (1985) demonstrated classification of individual trees into conifers and broadleaves partly based on airborne laser intensity. Since then the use of laser intensity has been little explored. This is mainly because of lack of methods for radiometric calibration of intensity values (Kaasalainen et al., 2005). However, recently some authors have tested intensity features for tree species classification (Brandtberg, 2007; Brandtberg et al., 2003; Holmgren et al., 2008; Holmgren & Persson, 2004; Moffiet et al., 2005; Reitberger et al., 2008) and for discerning age classes (Farid et al., 2006a,b) as well as land-cover classes (Brennan & Webster, 2006) where deciduous and coniferous forest were treated as separate classes. Despite the lack of calibration methods, intensity features derived from ALS data may improve classification (e.g. Brandtberg et al., 2003; Holmgren et al., 2008). As methods for calibration of the intensity mature, the usefulness of intensity used for individual tree species classification may increase.

In species classification, features derived from the laser height distribution, such as the mean height of the laser echoes, could be used directly in the classification algorithm (e.g. Brennan & Webster, 2006) or as a scaled feature, for example normalized with tree height (Holmgren & Persson, 2004). In individual tree classification, independence of tree height is important, especially in forests where tree height distributions differ between species. To ensure this independence features should be scaled. Brandtberg (2007) normalized the 3D point cloud using estimated tree height to ensure independence. Holmgren and Persson (2004) used relative height features, i.e., laser height features divided by the laser estimated height, to separate Norway spruce and Scots pine. It should be noted, however, that it has so far not been tested if scaling methods really produce independence of tree height. Robust scaling may be important for practical applications covering large areas. In large forested landscapes, species-specific height distributions will vary in the landscape according to soil properties, management history, and a number of other factors. Hence, selection of robust and unbiased classification features is important.

The aim of this study was to identify candidate ALS-derived features suitable for classification of spruce and birch. In order to reach our aim, we (1) conducted an analysis of differences in (1a) structural- and (1b) intensity features between spruce and birch trees, and (2) tested the classification performance of candidate features.

2. Materials and methods

2.1. Study area

The study area is located in the southwestern corner of Østmarka forest reserve. The forest reserve is located a few kilometers outside Oslo in southeastern Norway (59°50′N, 11°02′E, 190–370 masl). The size of the forest reserve is about 1800 ha. No logging or other silvicultural treatments has been carried out since the 1940s. Today the forest appears with large within stand variation in ages and sizes of trees. The forest is dominated by Norway spruce (*Picea abies* (L.) Karst.) and is partly multilayered. Deciduous trees are found scattered in the landscape. Birch (*Betula* spp.) and aspen (*Poplus tremula* L.) are the most commonly occurring deciduous species. An adjacent area outside the reserve was also included to cover managed forest in younger and intermediate age classes in the study.

2.2. Field data

During summer 2003, 20 circular field plots (0.1 ha) in the reserve and eight plots just outside the reserve were established. The plots were subjectively selected. The plots inside the reserve were selected according to three criteria, i.e., (1) they should be spruce-dominated, (2) have multiple canopy layers, and (3) be located on gentle terrain slopes. These field data were also used in studies by Solberg et al. (2006) and Bollandsås and Næsset (2007). The plots outside the reserve were selected to cover productive forest in young and intermediate age classes.

On each sample plot, we callipered diameter at breast height (DBH) of all trees with DBH $\geq$3 cm and recorded polar coordinates of each tree from the plot center. The polar coordinates of the trees were determined using tape measure and a compass. The compass had a foresight and was attached to a tripod to reduce pointing errors. In addition a local correction of the deviation between magnetic and true north were applied. Plot center coordinates were determined using differential Global Navigation Satellite Systems (GNSS) by means of Global Positioning System (GPS) and Global Navigation Satellite System (GLONASS). Random errors reported from the post-processing combined with empirical experience reported by Næsset (2001) indicated an average error of 10 cm for the planimetric coordinates of the plot centers. For further details about the GNSS setup and post-processing, see Solberg et al. (2006) and Bollandsås and Næsset (2007).

Selection of sample trees on each plot was performed in three steps, i.e., (1) four sample trees where systematically selected being the first non-suppressed coniferous trees found going clockwise around the plot after passing each cardinal direction. (2) The second step was to select four coniferous trees among all social status classes, being the next tree to each of the first sample trees according to increasing azimuth from plot center, and (3) the last step was to sample all deciduous trees on the plot. In addition, we subjectively selected some deciduous trees outside, but close to the plot. The last step was accomplished to get a better balance between number of selected coniferous and deciduous trees. The tree with the longest distance to plot center was located 26.8 m from the center.

Tree height, height to crown base, and crown radius were measured on the sample trees. Crown radius was calculated as the average of radii measured in the four cardinal directions. Tree height was measured using a Vertex III hypsometer. A summary of characteristics of field measured spruce and birch trees appear in Table 1.

2.3. Airborne laser scanner data

ALS data used in this study were acquired 18 June 2005 under leaf-on conditions with the Optech ALTM 3100 sensor. The sensor operated

Table 1
Summary of field measurements of trees.

Tree species	Characteristic	n	Mean	Std	Min	Max
Norway spruce	Tree height (m)	209	17.6	8.6	1.8	33.8
	Stem diameter (cm)	209	23.7	12.9	1.7	51.0
	Crown radius (m)	209	1.5	0.6	0.5	2.9
	Crown base height (m)	209	4.2	3.7	0.0	16.1
Birch	Tree height (m)	203	12.1	6.4	1.6	29.1
	Stem diameter (cm)	203	14.1	9.2	2.1	39.5
	Crown radius (m)	203	1.4	0.7	0.3	4.2
	Crown base height (m)	194	5.8	4.4	0.0	18.9

with a laser pulse repetition rate of 100 kHz and a scanning frequency of 70 Hz. In total, eleven individual flight lines were flown to cover the field plots. Individual strips overlapped with about 15%. Average flight speed was 75 ms^{-1} at a mean altitude of 750 m a.g.l. The maximum scan angle of 20° yielded a swath width of about 260 m. Pulses transmitted at half scan angles that exceed 8° were excluded from the final dataset in order to eliminate erroneous edge points as ALS sensors with oscillating mirrors have less accurate determination of z and across track coordinates at the scan edge. These errors occur because of the difficulty of modeling the rapid deceleration and acceleration that occur when the mirror is turning. Hence, the total scan angle used was 16°. The beam divergence was 0.28 mrad which yielded an average footprint size of about 21 cm. The average point spacing was 0.37 m by 0.54 m which gave an average point density of 5.09 m^{-2}. The recorded mean point density inside the tree segments of the studied trees was 6.6 m^{-2} and the standard deviation was 3.2 m^{-2}. Point density variation is partly caused by overlapping flight lines. Using ALS data from overlapping flight lines are frequently used in operational forest inventory and is probably the only way to obtain species information over large areas in a "wall-to-wall"context. However, since the ALS is a sample device, the higher point density will only lead to a more precise determination of laser-derived features.

Initial processing of the data was accomplished by the contractor (Blom Geomatics, Norway). Planimetric coordinates (x and y) and ellipsoidal height values were computed for all echoes. One of the flight lines was flown perpendicular to the other flight lines and used in matching and correction for systematic errors between swaths. Ground points were found and classified using the progressive Triangular Irregular Network (TIN) densification algorithm (Axelsson, 1999) of the Terrascan software (Terrasolid Ltd., 2004). A TIN was created from the planimetric coordinates and corresponding heights of the laser echoes classified as ground points. The ellipsoidal height accuracy of the TIN model was expected to be around 20–30 cm (e.g. Hodgson & Bresnahan, 2004; Kraus & Pfeifer, 1998; Reutebuch et al., 2003). The heights above the ground surface were calculated for all echoes by subtracting the respective TIN heights from all echoes recorded.

Older ALS systems (e.g. Optech ALTM 1210) typically record two echoes for each pulse, i.e., first and last echoes. The ALTM 3100 sensor used in this study is capable of recording up to four echoes per pulse. To separate different echoes acquired by such a system there has to be a certain time interval between the echoes. This time interval is known as the vertical resolution (Baltsavias, 1999). The vertical resolution for the sensor used in this study varies between 2.1 m for the two first echoes to 3.8 m for the other echoes. If four echoes are detected by the ALTM 3100 sensor, they are labeled as "first echo of many", "second echo", "third echo", and "last echo of many". If there are three echoes, they are labeled "first echo of many", "second echo", and "last echo of many". Furthermore, if two echoes are recorded they are labeled "first echo of many" and "last echo of many". Finally, if only one echo is recorded it is labeled as a "single echo". "Single echoes" are registered if the distance between the first echo and the last echo is less than 2.1 m or if it is not enough energy to trigger a second echo.

In this study, ALS data were delivered by the contractor as two datasets to be as close to the structure of the data provided by the ALTM 1210 sensor as possible, i.e., with "first echoes of many" plus "single echoes" as one dataset and "last echoes of many" plus "single echoes" as a second dataset. The use of two echoes, i.e., first and last, is common in operational ALS-assisted forest inventories in Norway (Næsset, 2004a). However, in this particular study, we split the two datasets based on spatial coordinates of the echoes into three different datasets containing the individual echo categories, i.e., (1) "first echoes of many", (2) "single echoes", and (3) "last echoes of many". The echo categories were denoted as "FIRST", "SINGLE", and "LAST", respectively. These three echo categories were used in the analysis. The relations between echoes of the same pulse have been outlined as important information to separate tree species (Brandtberg, 2007) and have been tested in tree species classification (Holmgren & Persson, 2004). However, given the structure of the data delivery in the present study, it was not possible to reconstruct the original data structure and tie the different echoes of each pulse to each other. Each echo category was therefore treated separately.

The intensity values used in this study were the uncalibrated intensity as recorded by the sensor. The intensity data recorded by ALS are noisy and will vary with target and sensor properties. Several studies have explained this noise by varying reflectivity with different directions of different target surfaces (Song et al., 2002; Wotruba et al., 2005). Hence, intensity of a target as measured by ALS will change with the scan angle of the emitted pulse (Kaasalainen et al., 2005). This could be adjusted for, but we did not have sufficient information to apply such a radiometric correction of the raw intensity values.

2.4. Computation of features of individual tree segments

In the present study, we did not use any crown delineation algorithm to identify the individual tree segments. Instead, we computed the crown radius for each tree as the mean of the field

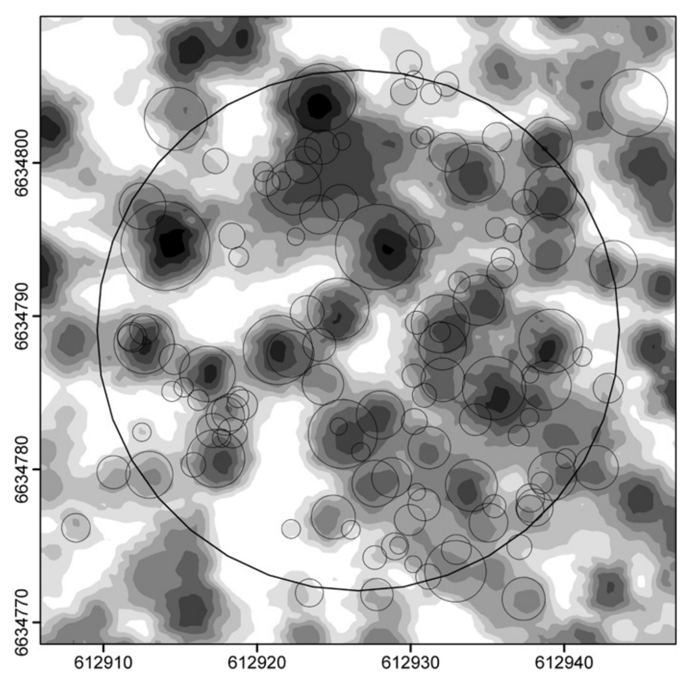

Fig. 1. Example of crown map (plot #14) showing the heterogeneous structure of the forest which lead to a number of overlapping crowns. The crown shapes are draped above a canopy surface model interpolated from laser echoes.

measured radii in the four cardinal directions and this quantity was used to buffer the field-measured stem position producing circular crown outlines (Fig. 1).

After having generated the circular tree segments, each laser echo was assigned to its corresponding tree crown. For trees with overlapping crowns, echoes in the overlapping zone were assigned to the tallest tree. Since laser measurements always will underestimate true tree height (Gaveau & Hill, 2003), echoes with higher *z*-value than the actual field-measured tree height were deleted. This correct for errors caused by erroneous positions and the assumption of circular crowns.

In area-based forest inventory where the ALS-related metrics are derived from the laser height distribution of a plot or certain target area (cf. Næsset, 2002), laser echoes between the ground surface (the TIN surface) and a threshold of, say, 2 m, are often considered as echoes from stones or under-vegetation and thus not included in analyses of the canopy (Næsset, 2002; Næsset & Bjerknes, 2001). A Ground Threshold Value (GTV) of 2 m is in accordance with the work by Nilsson (1996). In forestry, parameters like diameter, age, and basal area are most commonly registered at breast height, i.e., the point of the stem located 1.3 m above ground. We argue that breast height should be used as the GTV in individual tree assessment based on ALS data for consistency, unless there are specific reasons not to, for example when *a priori* knowledge of the height of the under-vegetation exist (Holmgren, 2004). In the multi-layered forest in our study area we also wanted to keep as much information as possible about the small trees. Hence, in the present work we used breast height (1.3 m) as the GTV.

For each tree segment, we used the point cloud to calculate four groups of structural features, i.e., (1) Normalized Height Features (NHF), (2) Canopy Penetration Depth (CPD), (3) Other Height Features (OHF), and (4) Crown Density Features (CDF). We also used one group of intensity features, i.e., Laser Intensity Features (LIF). From the echo height distribution we computed maximum (HMAX), mean (HMEAN), and height percentiles at 10% intervals (H10, H20, …., H80, H90) for each segment. These features were scaled to produce NHF and CPD (Eqs. (1)–(2)) described in Section 2.5. We selected the H10, H50, and H90 percentiles for further analysis. In addition we computed Other Height Features (OHF) including kurtosis (HKURT) and skewness (HSKEW) of the laser height distributions. Furthermore, standard deviation (HSTD), scaled according to Eq. (1), and coefficient of variation (HCV) for the laser height values were calculated in the OHF group. The features were calculated from all echoes above the GTV and for separate echo categories, i.e., FIRST, SINGLE and LAST.

Crown density features (CDF) were calculated in accordance with canopy density calculation in area-based forest inventory (Næsset, 2004c). The crown was divided into vertical crown layers by dividing field-measured tree height minus the GTV value (1.3 m) into 10 layers of equal height. Crown density was calculated for each echo category as the proportion of echoes above layer number 0 (>GTV), 1, …, 9, to total number of echoes in that category for each tree, and these densities were denoted as D0, D1, …, D9. D1, D5, and D9 were selected for further analysis.

Laser intensity features (LIF) derived for each individual tree were maximum intensity (IMAX), mean intensity (IMEAN), median intensity (IMEDIAN), kurtosis (IKURT), skewness (ISKEW), standard deviation (ISTD), and coefficient of variation (ICV) for echoes above GTV for the separate echo categories.

2.5. Scaling of laser height features

As stated above, two different scaling methods were applied in order to ensure independence of tree height and to utilize laser height features (i.e., HMAX, HMEAN, H10, H20, …., H90, HSTD) in species classification. In our study, two scaling approaches were used, i.e., (1) normalized with tree height to produce NHF (Eq. (1)) and (2) transformed to CPD using tree height (Eq. (2)):

$$\mathrm{NHF} = \frac{\mathrm{LHF}}{h} \tag{1}$$

where

NHF laser-derived height feature normalized with field-measured tree height,
h field-measured tree height,
LHF laser-derived height feature, i.e., HMAX, HMEAN, H10, H20, …., H90, HSTD.

$$\mathrm{CPD} = h - \mathrm{LHF} \tag{2}$$

where

CPD laser-derived height feature scaled to crown penetration depth,
h field-measured tree height,
LHF laser-derived height feature, i.e. HMAX, HMEAN, H10, H20, …., H90.

2.6. Tree height and laser echo categories

The forest in the Østmarka forest reserve is heterogeneous with complicated structure and a number of overlapping tree crowns (Fig. 1). The spatial distribution and size of the trees will influence on the number of echoes returned from inside a tree segment. In addition, not all the field-measured trees will have echoes of all categories. For short trees, FIRST and LAST echoes in particular will be limited in number because of the limited vertical resolution of the ALS sensor. In order to calculate all the defined variables for a tree, at least three echoes above GTV in each echo category are needed. This requirement reduced the number of trees subject to analysis significantly. We therefore analyzed two separate datasets, i.e., (1) one containing trees hit by at least three echoes of each category above GTV and (2) one with those trees not satisfying the criteria of the first dataset, but with at least three SINGLE echoes above GTV for each tree. The first dataset comprised 201 trees and was labeled Large Trees because it on average contained higher trees (Table 2) than the Small Trees dataset of 176 trees. The field-measured tree height distributions of each species for the two tree categories are displayed in Fig. 2. For the two datasets, we computed and reported the proportions of echoes in the different echo categories (FIRST, SINGLE, LAST) as observed in the sample trees above and below GTV (Table 3). The proportions of echoes were computed relative to the sum of FIRST and SINGLE echoes. This information is interesting in evaluating the split into tree categories and to assist evaluation of crown density features.

Table 2
Summary of number of trees and heights in the two tree categories used in the analysis.

Tree categories	Tree species	n	Tree height (m)			
			Mean	Std	Min	Max
Small Trees	Spruce	78	9.6	5.5	2.6	27.8
	Birch	98	8.5	4.5	2.4	24.0
Large Trees	Spruce	119	23.8	4.2	12.0	33.8
	Birch	82	17.6	4.3	9.2	29.1

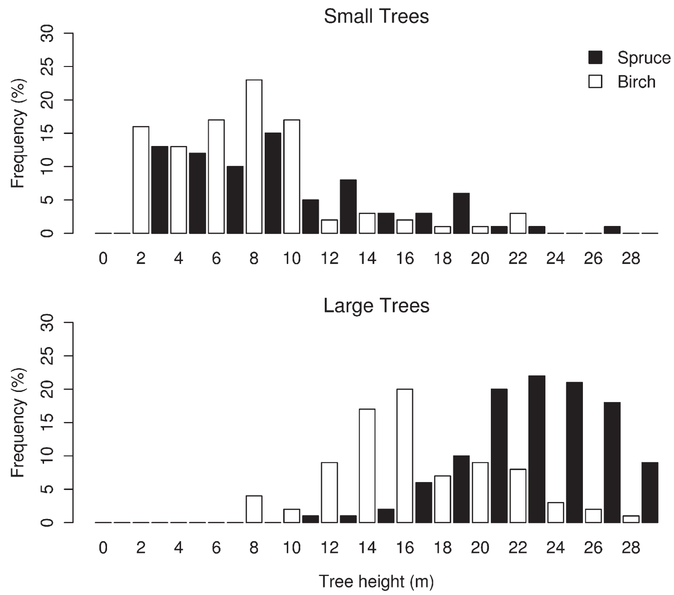

Fig. 2. Histogram of tree height distribution in the two datasets labeled Small Trees and Large Trees. The dataset Large Trees contains trees hit by at least tree pulses with all echo categories and the dataset Small Trees contains the remaining trees with at least tree pulses with echoes of the SINGLE category.

2.7. Analysis of differences between tree species

Generally, a laser feature can be used for species classification if it differs significantly between species (e.g. Brandtberg et al., 2003; Holmgren & Persson, 2004). Instead of only analyzing differences in mean values using *t*-tests or analysis of variance we incorporated tree heights into our analysis. Hence, we computed a linear regression model including tree species and field-measured tree height as covariates and the specific laser features as the response variable. Tree species was included as a dummy variable. Such analyses are often refereed to as analysis of covariance (ANCOVA). The full model (Eq. (5)) was estimated with ordinary least square regression using the R stats package (R Development Core Team, 2007). In addition, simpler models were estimated by removing one (Eq. (4)) or two (Eq. (3)) of the latter terms of the full model (Eq. (5)). All together three different models were estimated:

$$\mathrm{LF} = \beta_0 + \beta_1 SP \tag{3}$$

$$\mathrm{LF} = \beta_0 + \beta_1 SP + \beta_2 h \tag{4}$$

$$\mathrm{LF} = \beta_0 + \beta_1 SP + \beta_2 h + \beta_3 h{*}SP \tag{5}$$

where

LF laser-derived feature, i.e., all features in the five feature groups (NHF, CPD, OHF, CDF, LIF),
h field-measured tree height,
SP dummy variable for tree species. $SP=1$ if spruce and $SP=-1$ if birch.

The "best" model of the three estimated, was selected using F statistics, also known as the partial F-test. Simpler models, i.e., fewer parameters estimated, were selected if they did not have significantly ($p \leq 0.05$) lower explanatory power than more complex models. The F statistics was computed with the *anova*-function of the R stat package (R Development Core Team, 2007) and it was computed by dividing the difference in model residual sum of squares by the ratio of model residual sum of squares by degrees of freedom for the more complex model (Eq. (6)). In the complex model, one parameter more than in the simple model is estimated.

$$F = \frac{\mathrm{RSS}_1 - \mathrm{RSS}_2}{\mathrm{RSS}_2 / \mathrm{DF}_2} \tag{6}$$

where

RSS_1 residual sum of squares of simpler model, e.g. Eq. (4),
RSS_2 residual sum of squares of complex model, e.g. Eq. (5),
DF_2 degrees of freedom of complex model, e.g. Eq. (5).

If the best model selected based on Eq. (6) was the full model (Eq. (5)) the estimated β_0 is the intercept, β_1 is the change in intercept for species (plus for spruce and minus for birch), β_2 is the estimated slope for tree height, and β_3 is the change in slope for tree species (plus for spruce and minus for birch). The significance of the model terms (SP, h, $h*SP$) was tested using an F-test. The null hypothesis tested was that the betas (β_1, β_2, β_3) were equal to zero when all other terms were included in model, i.e., using adjusted sum of squares — also called Type III-test. In order to compare variance explained for different features, we compute single term coefficients of variation using adjusted sum of square for the single term divided by the sum of single term sum of squares plus residual sum of squares, i.e.,

$$\eta^2_{\mathrm{effect}} = \frac{\mathrm{SS}_{\mathrm{effect}}}{\mathrm{SS}_{\mathrm{total}}} \times 100 \tag{7}$$

where

η^2_{effect} eta-squared for effect, i.e. tree species (SP), tree height (h) or interaction ($h*SP$),
$\mathrm{SS}_{\mathrm{effect}}$ adjusted sum of squares for single model terms, i.e. tree species (SP), tree height (h) or interaction ($h*SP$),
$\mathrm{SS}_{\mathrm{total}}$ adjusted sum of squares for all model terms i.e. tree species (SP), tree height (h) or interaction ($h*SP$), and the error term.

In variance analysis such measures are often referred to as the correlation ratio or eta-squared (η^2_{effect}) (Kline, 2004). Eta-squared will sum to 100 for all model terms. However, the sum of eta-squared (η^2_{effect}) for all terms is different from the coefficient of determination (R^2) although both are measures of explained variability. The reason for this difference is that in computation of η^2 adjusted sum of square is used and in computation of R^2 sequential sum of square is used. We used eta-squared for the tree species term (η^2_{SP}), or as referred to in this study, the proportion of variability explained by tree species, to identify candidate features. Candidate features should have a high proportion of variability explained by tree species (η^2_{SP}) and explained variability should be higher for tree species than by other model terms.

In order to test classification performance of candidate features (objective 2), classification was carried out using Linear Discriminant

Table 3
Proportion (%) of echoes relative to the sum of FIRST and SINGLE echoes for the two tree categories (Large Trees and Small Trees) split on tree species and above and below ground threshold value (GTV = 1.3 m).

Tree species	Echo category	Large Trees		Small Trees	
		H>=GTV	H<GTV	H>=GTV	H<GTV
Norway spruce	FIRST	35	0	12	0
	SINGLE	62	3	81	7
	LAST	21	20	5	10
Birch	FIRST	41	0	25	0
	SINGLE	52	7	65	10
	LAST	18	26	2	26

Analysis (LDA). The estimation was conducted using the *lda*-function of the R package MASS (Venables & Ripley, 2002) using equal prior probabilities and full cross validation. From the resulting error matrix, accuracy was computed for each tree species and for the overall classification. Classification was carried out for single candidate features. Features with low overall accuracy were removed from the set of candidate features. Finally, classification was carried out for the combination of the "best" candidate feature in each feature group and for separate echo categories.

In addition to the analysis described above, we also visualized the distribution of normalized laser heights and the raw intensity values by density plots. The plots will identify differences in the height and intensity distributions between species. Density estimation is a method used to estimate probability density functions from sample data. Density estimates are very useful in exploration and presentation of data (Silverman, 1986). In this study, we used the kernel estimator to estimate the density function. The density function was computed with the R stats package (R Development Core Team, 2007) using a Gaussian kernel and bandwidth selection using the Silverman's "rule-of-thumb" (Venables & Ripley, 2002). The kernel density plots will produce a better visualization of the height- and intensity distributions than histograms, but interpretation will be the same.

3. Results

The results of the analysis of covariance (ANCOVA) (Eqs. (3)–(5)) and model selection procedure (Eq. (6)) are summarized in Table 4. The analysis revealed that many of the computed laser features differed significantly between tree species. In 52 of 72 estimated models, tree species was a significant ($p<0.05$) explanatory variable of the specific laser feature analyzed. However, selected models also demonstrated that analyzed laser features were influenced by tree height. For the 72 laser features tested, 41 models included the covariate (tree height). Among these 41 models, 13 also included the interaction term. Comparing proportion of variability explained by tree species (η^2_{SP}) in the selected model and the simple one-way ANOVA model (Eq. (3)) illustrates that tree height would influence selection of candidate variables if we did not considered tree height as a covariate (Fig. 3).

3.1. Differences in structural features between tree species (Objective 1a)

The height distributions of laser echoes for different species, echo categories, and tree height categories (Large Trees and Small Trees) are visualized in Fig. 4. The normalized laser height features (NHF) computed from FIRST and SINGLE echoes for birch trees were larger than for spruce trees (Table 4). Conversely, NHF computed from LAST echoes were smaller for birch trees than for spruce trees. The highest proportion of variability explained (η^2_{SP}) obtained for tree species from NHF was 11% for Large Trees and 17% for Small Trees. However, a similar or higher proportion of the variation was explained by tree height. Moreover, we also carried out the ANCOVA with height features scaled as crown penetration depth (CPD) (Eq. (2)). CPD from FIRST and SINGLE echoes were significantly deeper for spruce compared to birch (Table 4). In the CPD group, only features not influence by tree height, i.e., CPD computed from SINGLE echoes and

Table 4
Summary of analysis of covariance (ANCOVA)[a].

Laser feature[b]	Large Trees																		Small Trees					
	FIRST						SINGLE						LAST						SINGLE					
	SP		*h*		*h*SP*		*SP*		*h*		*h*SP*		*SP*		*h*		*h*SP*		*SP*		*h*		*h*SP*	
HMAX (NHF)	−4	**	+3	*			−3	*	+3	*			+0	ns	**+13**	***			−6	**	+8	***		
HMEAN (NHF)	−6	***	+6	***	+3	**	**−11**	***	**+11**	***			+7	***	**+15**	***			**−17**	***	**+15**	***		
H10 (NHF)	−7	***	+3	*	+4	**	−5	***	+8	***			+5	***	+7	***			**−12**	***	**+11**	***		
H50 (NHF)	−5	***	+5	**	+3	**	−9	***	+7	***			+6	***	**+13**	***			**−17**	***	**+17**	***		
H90 (NHF)	−2	*	+4	**			−9	***	+6	***			+1	ns	**+10**	***			−9	***	+9	***	+2	*
HMAX (CPD)	**+11**	***					+4	**					+1	ns					+3	*	+2	*		
HMEAN (CPD)	+6	***	+9	***	−3	**	**+26**	***					+1	ns	**+25**	***	−2	**	+9	***	**+31**	***		
H10 (CPD)	+5	***	**+11**	***	−3	**	**+16**	***					+2	*	**+31**	***	−3	**	+5	***	**+37**	***		
H50 (CPD)	+5	***	+5	***	−3	**	**+19**	***					+1	ns	**+17**	***	−3	**	**+11**	***	**+25**	***		
H90 (CPD)	+2	*	+3	*			**+18**	***					−1	ns	+4	**			+6	***	+8	***		
HSD (NHF)	**+10**	***	−1	ns	−7	***	+0	ns	−9	***			+2	ns	−0	ns	−2	*	+7	***	−5	**		
HCV	**+11**	***	−2	*	−8	***	+1	ns	−9	***			−6	***	−3	**			**+11**	***	−7	***		
HKURT	**−13**	***	+2	*			**−14**	***					−0	ns	+3	*			−1	ns				
HSKEW	+7	***	−2	*			**+18**	***					−4	**	−3	*			+2	ns	−7	***		
D1	+1	ns					**+12**	***					**+11**	***					+1	ns	**+16**	***		
D5	**−10**	***	+7	***	+6	***	+0	ns	+5	**			**+13**	***	+5	***			−2	*	**+27**	***		
D9	+1	ns					−20	***	+6	***			**+17**	***					−7	***	**+19**	***		
IMAX	**−19**	***					−3	*					+1	ns					+2	ns	+2	ns	−4	*
IMEAN	**−18**	***					−1	ns					**+19**	***	−6	***			+2	ns	+0	ns	−5	**
IMEDIAN	**−14**	***					−1	ns					**+18**	***	−6	***			+2	ns	+0	ns	−5	**
ISD	−8	***					−3	*					+3	*					−0	ns	+6	**		
ICV	+2	ns					−2	ns					+2	ns					+0	ns	+5	**		
IKURT	−4	**					+1	ns					−5	***	+3	*			+4	**	+1	ns	−5	**
ISKEW	+2	*					−2	*					−11	***	+5	***			+0	ns				

The sign of the regression coefficients[c] variability explained by (η^2_{effect}) model terms, and the significant level[d] of the term for selected models are displayed for different tree height categories, echo categories, and model terms, i.e., tree species (*SP*), tree height (*h*), and the interaction term (*h*SP*). Model terms with higher variability explained (η^2_{effect}) than 10 appear in bold.

[a] The displayed models are the best ones (i.e. Eq. (3), Eq. (4), or Eq. (5)) selected according to Eq. (6).

[b] HMAX = maximum height of laser height distribution; HMEAN = mean height of laser height distribution; H10, H50, and H90 = 10, 50, and 90 percentiles of laser height distribution; HSD = standard deviation of laser height distribution; HCV = coefficient of variation of laser height distribution; HKURT = kurtosis of laser height distribution; HSKEW = skewness of laser height distribution. Abbreviations in parenthesis refer to scaling method, i.e. normalized height features (NHF) (Eq. (1)) or canopy penetration depth (CPD) (Eq. (2)). D1, D5, and D9 = crown densities corresponding to proportions of laser echoes above layer # 1, 5, and 9, see text for further details; IMAX = maximum value of laser intensity distribution.; IMEAN = mean value of laser intensity distribution.; IMEDIAN = median value of laser intensity distribution.; ISD = standard deviation of laser intensity distribution.; ICV = coefficient of variation of laser intensity distribution.; IKURT = kurtosis of laser intensity distribution.; ISKEW = skewness of laser intensity distribution.

[c] Plus (+) for species (*SP*) and interaction (*h*SP*) represent higher values for spruce compared to birch. Plus (+) for tree height (*h*) represent increasing values with increasing tree height.

[d] Level of significance: ns = not significant (>0.05); *<0.05; **<0.01; ***<0.001.

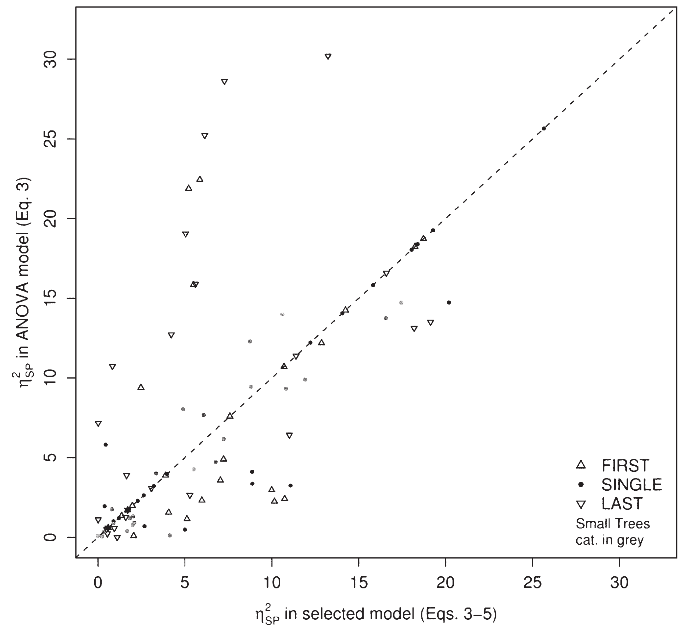

Fig. 3. Proportion of variability explained by tree species (η^2_{SP}) for different laser features in ANOVA model (Eq. (3)) compared to in selected ANCOVA model (Eqs. (3)–(5)). Laser features in the upper left of the plot have lower explained variability of tree species when tree height is introduced as covariate. Laser features in the lower right of the plot will explain more of the difference between tree species when the covariate is introduced. Laser features at the 1:1 line are features where the ANOVA model (Eq. (3)) is selected as the one with the significantly highest variability explained.

HMAX from FIRST echoes, had potential for tree species classification. The Small Trees category was highly influenced by tree height both within NHF and CPD.

The effect of the two different scaling methods is illustrated with proportion of variability explained by the tree species term (η^2_{SP}) in percentile (H10–H90) models (Fig. 5). The proportion of variability explained for percentiles derived from SINGLE echoes scaled to crown penetration depth (CPD) were on average 11% higher than the corresponding relative heights (NHF).

The normalized standard deviation (HSTD) and coefficient of variation (HCV) differed between the two species for FIRST echoes and FIRST and LAST echoes, respectively, in the Large Trees category (Table 4). For Small Trees, both HSTD and HCV differed between species. However, both features were always dependent on tree height in the Small Tree category. HCV was found to be as good as HSTD or better in terms of proportion of variability explained by the models. The analysis also revealed that HSTD and HCV in general were lower for birch trees for all echo categories.

Skewness (HSKEW) and kurtosis (HKURT) were found to have potential for tree species classification for the Large Trees category when computed from FIRST and SINGLE echoes (Table 4). Skewness and kurtosis for the FIRST and SINGLE echoes indicated that the distribution was more skewed, sharp, and a bit more shifted upwards for birch than for spruce (Table 4 and Fig. 4).

The differences in crown density between tree species were most pronounced for features computed from LAST echoes (Table 4, Fig. 6). For FIRST echoes, the largest differences were found in the intermediate parts and for SINGLE echoes the largest differences were found in the lower and upper part of the crown. Small Trees crown density features were highly influenced by tree height and were only statistically significant in the upper parts of the tree crown. Furthermore, it was also found that tree heights significantly influenced the values of most crown density features also for the Large Trees category.

3.2. Differences in intensity features between species (Objective 1b)

The estimated distributions of uncalibrated intensity for the two species for each echo category and for the two tree categories are plotted in Fig. 7. The main difference in the intensity distributions was between the echo categories. SINGLE echoes had higher intensities compared to FIRST and LAST echoes. Both FIRST and LAST echoes had approximately half the mean intensity values compared to SINGLE echoes, i.e., 56 and 41%, respectively. There was no clear difference

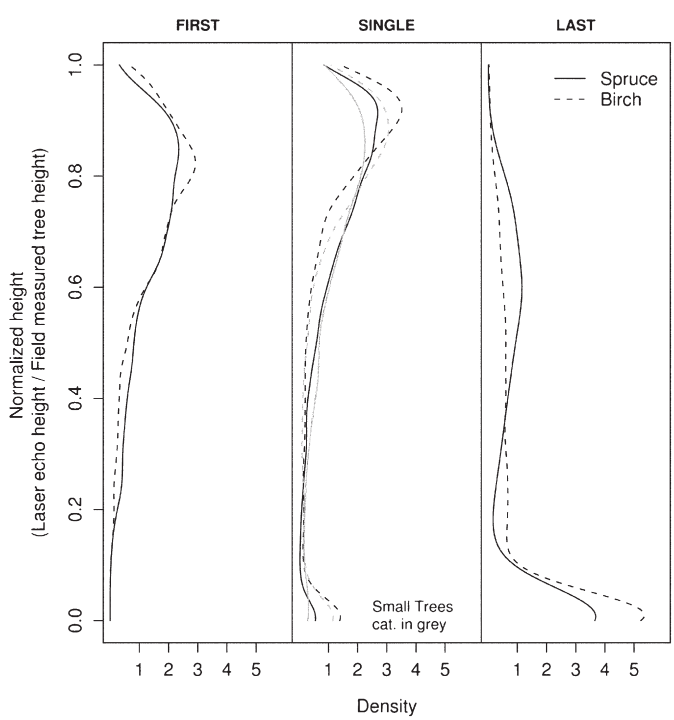

Fig. 4. Normalized laser height distributions, estimated as kernel density, for different tree species and echo categories for both tree categories. The Small Trees dataset is only represented by SINGLE echoes.

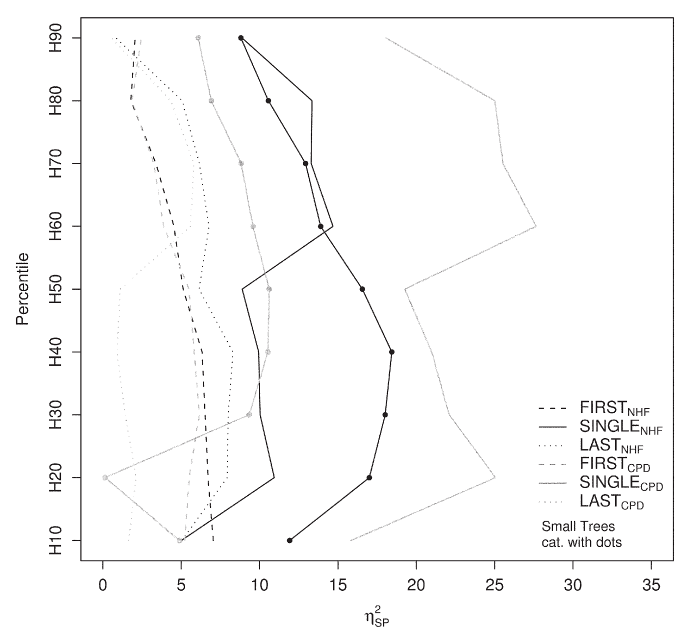

Fig. 5. Proportion of variability explained by tree species (η^2_{SP}) for different percentiles (H10–H90) and scaling methods, i.e., normalized height features (NHF) (Eq. (1)) and crown penetration depth features (CPD) (Eq. (2)), displayed for echo- and tree categories.

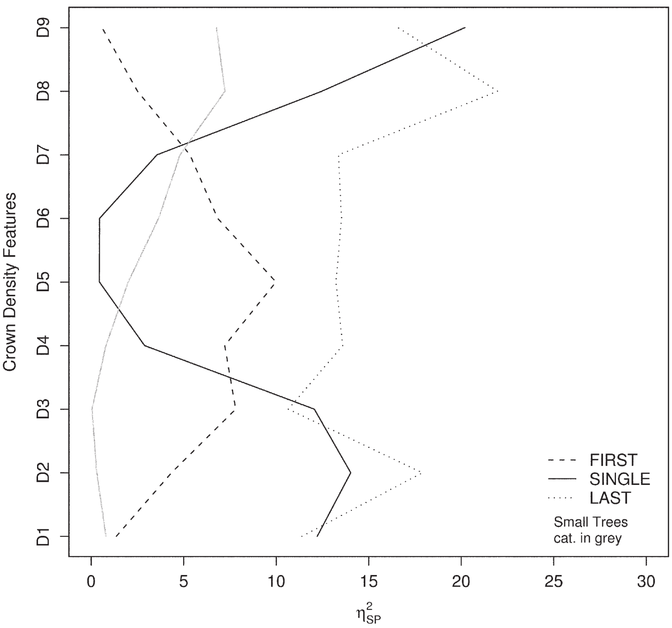

Fig. 6. Proportion of variability explained by tree species (η^2_{SP}) for different crown density features (D1–D9), echo- and tree categories. Crown densities are computed as the number of echoes of an echo category above a given vertical layer as a proportion of total number of echoes of that specific category, see text for further details.

between tree species in the density plots (Fig. 7). The ANCOVA (Table 4) revealed that laser intensity features were higher for birch trees than for spruce with exception of the LAST echoes where the opposite effect was observed. The largest proportions of variability explained were in intensity features from FIRST echoes (IMAX, IMEAN, IMEDIAN) and LAST echoes (IMEAN, IMEDIAN). Furthermore, features derived from the LAST echoes were significantly related to tree height. For Small Trees, none of the computed intensity features, except from IKURT, differed between the two species (Table 4).

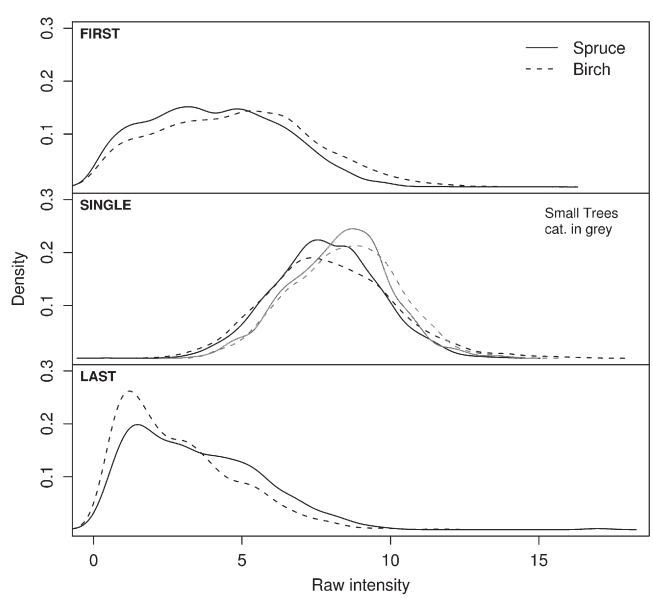

Fig. 7. Laser intensity distributions, estimated as kernel density, for different tree species and echo categories for both tree categories. The Small Trees dataset is only represented by SINGLE echoes.

Table 5
The three features[a] within tree categories, echo categories, and feature groups[a] with the highest proportion of explained variability (η^2_{SP}) for tree species in ANCOVA model.

Feature groups[b]	Large Trees			Small Trees
	FIRST	SINGLE	LAST	SINGLE
NHF	H10(59)	*HMEAN(60)*	HMEAN (74)	***HMEAN(64)***
	HMEAN(58)	H50(61)	H50(74)	***H50(64)***
	H50(55)	H90(61)	H10(70)	*H10(62)*
CPD	*HMAX (61)*	***HMEAN(75)***	H10(58)	H50(66)
	HMEAN(71)	***H50(74)***	H50(28)	HMEAN(65)
	H50(72)	***H90(69)***	HMEAN(52)	H90(64)
OHF	***HKURT(70)***	***HSKEW(70)***	**HCV(69)**	***HCV(65)***
	HCV(57)	***HKURT(72)***	HSKEW(66)	HSD(63)
	HSD(55)	HCV(55)	HSD(53)	HSKEW(56)
CDF	*D5 (58)*	***D9(67)***	***D9(67)***	D9(58)
	D1(61)	***D1(70)***	***D5(77)***	D5(52)
	D9(54)	D5(60)	*D1(65)*	D1(55)
LIF	***IMAX(73)***	ISD(55)	***IMEAN(67)***	IKURT(51)
	IMEAN(70)	IMAX(58)	*IMEDIAN(66)*	IMEDIAN(55)
	IMEDIAN(66)	ISKEW(59)	*ISKEW(65)*	IMEAN(53)

Overall accuracy of classification for single features is shown in parenthesis. Italic letters indicate that variability explained by tree species (η^2_{SP}) is greater than 10 and no other model term has higher explained variability ($\eta^2_{\bar{h}}, \eta^2_{\bar{h}*SP}$). Bold letters indicate candidate features having both high η^2_{SP} for tree species and high overall accuracy.
[a] Symbols explained in Table 4.
[b] NHF = normalized height features, CPD = crown penetration depth, OHF = other height features, CDF = crown density features, and LIF = laser intensity features.

3.3. Classification performance of candidate features (Objective 2)

The overall classification accuracies of the three features with highest proportion of variability explained by tree species (η^2_{SP}) in the five feature groups (NHF, CPD, OHM, CDF, and LIF) are presented in Table 5. Laser features with proportions of variability explained by tree species (η^2_{SP}) higher than 10 and where a greater proportion of variability was explained by tree species than by other model terms are presented in italics. Features presented in bold were considered as candidate features. In addition to meeting the criteria for proportion of variability explained by tree species (η^2_{SP}), the candidate features had high (>67%) overall classification accuracies.

Combining the candidate features with highest proportions of variability explained by tree species (η^2_{SP}) in each feature group and echo category increased the overall accuracy obtained for the Large Trees category. The combination of candidate features yielded an overall accuracy of 88% for Large Trees and 64% for Small Trees (Table 6).

4. Discussion and conclusions

4.1. Materials and methods

In this study, the main focus was on identifying candidate laser-derived features suitable for discriminating between coniferous

Table 6
Classification performance for a combination of features selected.

Tree categories	Features selected[a]			Classification accuracy (%)		
	FIRST	SINGLE	LAST	Spruce	Birch	Overall
Large Trees	HKURT IMAX	HMEAN(CPD) HSKEW D9	HCV D9 IMEAN	93.3	81.7	88.6
Small Trees		HMEAN(NHF) HCV		57.7	68.4	63.6

The features are selected from the candidate features (Table 5) having the highest (η^2_{SP}) in each feature group[b], echo category, and tree category.
[a]Symbols explained in Table 4.
[b]NHF = normalized height features, CPD = crown penetration depth, OHF = other height features, CDF = crown density features, and LIF = laser intensity features.

(spruce) and deciduous (birch) species. The study area is located in a forest reserve, and the tree height distributions observed in such a forest are likely to be different from those found in a managed forest. However, we found the data suitable for this study because datasets with large variation in tree size and spatial distribution of trees may provide a better basis for selecting robust laser features for species classification compared to less complex forests.

A possible source of error in the analyses are related the matching of field and laser data. The quality of this matching is dependent on the accuracy of the field measured tree coordinates and the assumption of circular crowns. However, the assumption of circular crown outlines as measured and reconstructed from field data will probably be more accurate than an outline produced by a segmentation algorithm in a relatively complex forest like the current. Moreover, tilting stems will offset the tree top positions relative to the measured positions registered in breast height using compass and measure tape. All these positional errors and errors in determining the true crown outline may cause commission of echoes from neighboring trees and omission of echoes from the tree in question. If there are between species commission and omission errors, they will tend to even out the differences in echo distributions between species. Since spruce is the most frequently occurring species in the study area, it is likely that echo distributions of birch trees will be more similar to echo distributions of spruce trees. Hence, computed features will be more similar between species. Therefore, identified candidate features probably are robust features not affected by these commission and omission errors.

4.2. General remarks on laser features and tree height scaling

This study has demonstrated that there are significant differences in many laser-derived features between spruce and birch. Therefore, many laser features may contribute to an improved tree species classification of individual trees based on ALS data. From the different types of features considered, i.e., normalized height features, canopy penetration features, crown density features, and uncalibrated laser intensity features, we identified laser features suitable to discriminate between the two species (Table 5). In the identification of features both echo category and tree size category were important. A specific type of feature may work well for species discrimination when it is computed for a certain echo category, but provide little or no useful information when computed from other echo categories. The identified candidate features varied also highly between tree categories (Large Trees and Small Trees).

We also found that many laser-derived features are affected by tree height. The relationship between laser derived features and tree height may also be linked to other properties which are related to tree height, e.g. size and shape (i.e. allometry) and the interior structure of the tree crown. Thus, changes in laser features with increasing tree heights will occur for both laser height features and laser crown density features, but to a smaller degree for laser intensity features. Therefore, discriminating between species based on structural properties derived from ALS data may be challenging in a forest where different species have different height distributions. *A priori* knowledge of forest structure and variation in species may therefore be important. Laser height features used must be scaled, trees stratified into height classes, or tree heights must be included in a classification algorithm. The two simple scaling methods applied in this study, i.e., normalization with tree heights and canopy penetration depth, failed to provide independence of tree height in most cases. Selected candidate features for Large Trees were only selected from crown penetration depth scaling. From the normalized height features often used in individual tree species classification no features was selected for the Large Tree category. However, if we had based our selection on the ANOVA model, such features might have been selected (Fig. 3). The overall accuracy of normalized HMEAN computed from LAST echoes was 74% (Table 5) and were among the highest in this study. However, the proportion of variability explained was 7% for tree species (η^2_{SP}) and 15% for tree height (η^2_{h}) (Table 4).

4.3. Structural features

The main differences between spruce and birch in general are the rounder (spherical) crowns of birch compared to the more conical crowns of spruce. In addition, the higher crown base height and allocation of biomass higher up in the crowns are typical for many deciduous tree species. These two differences were also expressed in the laser-derived features, see illustration in Fig. 8. First, the values of laser features computed from FIRST and SINGLE echoes revealed that echoes from these categories were reflected higher in birch trees than in spruce trees. The plausible explanation for this is the differences in crown shape between the species. It is also likely that other crown structural characteristic influenced on the echo distributions, such as crown density, leaf area, and leaf orientation (Gaveau & Hill, 2003). Secondly, the higher proportion of LAST echoes in the crown of spruce trees may be explained by the relatively lower crown base of spruce. In addition to having lower crown base, spruce trees also have a larger proportion of the crown located at a lower level in the tree. Both the differences in crown base height and crown biomass distribution will tend to allow more LAST echoes to penetrate below GTV for birch trees instead of being recorded in the canopy.

The 1–2 cm long needles of spruce in comparison to the ca 5–6× 5 cm plane birch leaves is another obvious difference that influences the crown structure. ALS data are influenced by the vertical distribution of biomass/leaf area (Coops et al., 2007; Magnussen & Boudewyn, 1998). Hence, the higher number of echoes in the upper crown of birch trees may also be attributed to denser and more compact tree crowns of this species. This effect is also expressed by the smaller variation in height of laser echoes in birch trees described by standard deviation and coefficient of variation. Especially SINGLE echoes were located at a point relatively higher up in birch crowns compared to spruce trees (Fig. 4). However, spruce had a higher portion of SINGLE echoes than birch (Table 3). This may be attributed

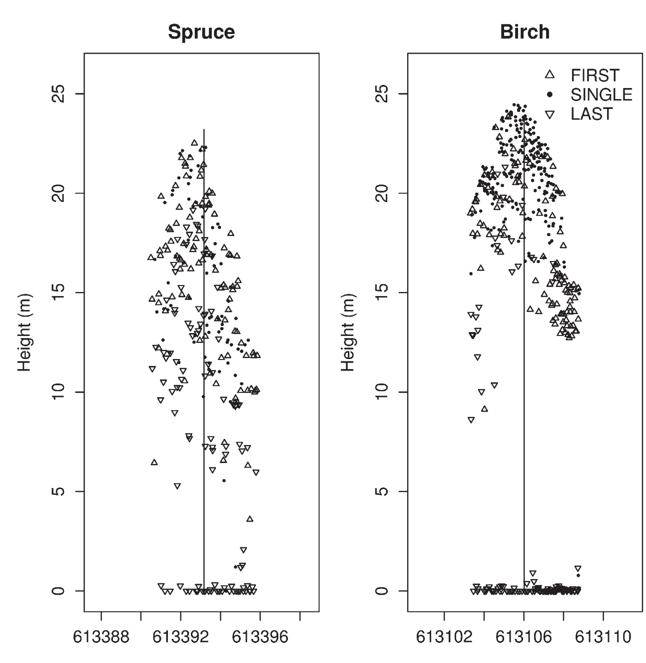

Fig. 8. Echoes of different categories plotted for two individual trees of spruce and birch.

to the fact that for spruce trees more echoes are located at a point where no additional echoes will be recorded, i.e., near the stem where no further penetration can be expected. In addition, the reflectivity properties of canopy elements, i.e., foliage, bark, and stem, will influence the distribution of laser echoes. In the wavelengths typically used by ALS sensors birch has higher reflectivity than spruce (Kuusk, A. pers comm.). Hence, FIRST and SINGLE echoes will tend to be recorded higher in the crown for birch trees.

In the Small Trees category only SINGLE echoes were observed. The main reason for this is probably the limited vertical resolution (2.1 m) of the laser sensor used. Another factor which will influence on the probability of reflecting three echoes or more of each category from an individual tree, which is the criteria for Large Trees, is the tree crown diameter. Hence, number of echoes will be low in the Small Trees category as a result of the limited vertical resolution and small crown diameters. Our analysis showed that SINGLE echoes were found higher in birch trees than spruce trees. This pattern coincides with what we found for the Large Trees category. In addition, it is important to notice the higher impact of tree height on laser height features computed from the Small Trees category. The large impact of tree height in this tree category resulted in quite few selected candidate features and made the selection of candidate features less convincing.

4.4. Intensity features

Among the intensity features, we found that the uncalibrated intensities from the FIRST echoes were the only ones that carried information useful for species discrimination. It seems that the uncalibrated intensities of FIRST echoes mostly are functions of the canopy reflectance of trees. Reflection from birch tends to be higher than for spruce for all canopy elements, i.e., stem, branches and leaf/needles, in the wavelength used by the current sensor (1064 nm) (Kuusk, A. pers comm.). The FIRST echoes are also likely to be less influenced by the biomass than subsequent echoes. The intensity of the LAST echo will be influenced by reflection and absorption higher up in the crown, and thus a higher intensity of e.g. the FIRST echo will tend to result in a lower intensity of LAST echoes, as we observed in this study. However, Reitberger et al. (2008) found that the mean intensity of laser echoes inside a tree produced higher classification accuracies than mean intensity of the upper 10% of the crown, but they did not distinguish between echo categories. A high proportion of reflections from the top of a tree will most likely be SINGLE echoes and hence the intensity will be higher and less different between species.

The advantage of intensity features computed from FIRST echoes is that they are independent of tree heights, at least for Large Trees, which we found not to be the case for the majority of the other derived features. We expected that intensity of SINGLE echoes of the Small Trees would be quite similar to FIRST echoes of the Large Trees, i.e., that the intensity primarily would be a function of species reflectivity. However, we found that intensity features were of little value for classification of spruce and birch when tree heights were <5–10 m. The difficulties of distinguishing between young conifers and young broadleaves were also reported by Schreier et al. (1985).

A large variability was inherent in the uncalibrated intensity values we used, and just a small portion of this variability seemed to be attributed to differences between species. Radiometric calibration of ALS intensities is not yet common practices in classification studies because of lack of appropriate methods (Boyd & Hill, 2007; Kaasalainen et al., 2005). Factors such as variable scan angle and flying altitude, atmospheric attenuation, and lack of stability of emitted pulse energy introduce noise to the recorded intensities. Using radiometric calibrated intensities instead of the raw intensities may yield less noise in the computed intensity features. Hence, radiometric calibrated intensities features may be more suited to distinguish between tree species.

4.5. Selected candidate features

We found that normalized height features were of little value in classification of larger trees, opposed to other studies. For example, Brandtberg et al. (2003) found that the normalized maximum height from first echoes had the highest overall tree species classification accuracy in a deciduous forest in eastern USA. In a Swedish study (Holmgren & Persson, 2004), the 90 percentile calculated for all echoes within the crown produced the lowest overall accuracy of features selected. Normalized percentiles tended to produce a very low accuracy using waveform data under leaf-on conditions in Germany (Reitberger et al., 2008), but was the group with second highest overall accuracy in another study conducted in the same area (Heurich, 2006). The new scaling method proposed in the present study, i.e., the canopy penetration depth scaling, is promising as a method to scale laser height features.

The other height features included variability features such as standard deviation (HSTD) and coefficient of variation (HCV) and features describing the shape of the distribution, i.e., kurtosis (HKURT) and skewness (HSKEW). HCV was selected as a candidate feature from the LAST echoes for Large Trees and from the Small Trees category. It should also be noted that HCV always was higher ranked than HSTD. Holmgren and Persson (2004) selected normalized standard deviation from all laser echoes within the tree crown as a candidate feature and overall accuracy was in the lower end compared to other features in the study. Also in a German study the standard deviations produce the lowest overall accuracies of features considered (Heurich, 2006). Our results indicate that the coefficient of variation should be used rater than the normalized standard deviation. In the study by Brandtberg et al. (2003), both standard deviation and kurtosis were selected as candidate features from the first echoes. In our study, kurtosis from FIRST and SINGLE echoes are recommended as features in addition to skewness for SINGLE echoes. The descriptions which kurtosis and skewness provide of the laser height distribution seem to be important in tree species classification.

Crown density features from the intermediate and upper part of the crown for LAST echoes and in the upper and lower part of the crown for SINGLE echoes are suggested as candidate variables in the present study. In a study from Germany, CDFs computed from a dual recording sensor provided the highest overall tree species classification accuracy under leaf-on conditions (Heurich, 2006). However, CDFs derived from waveform data in the same study area did not perform as well (Reitberger et al., 2008). In other studies, measures of crown density have been defined as proportion of echoes traveling below GTV (Moffiet et al., 2005) or as the proportion of echoes found above crown base to the total number of echoes (Holmgren & Persson, 2004). In both these latter studies, such features were shown to be of great importance in species classification. Also in our study density features contributed significantly to the separation of spruce and birch when computed from appropriate echo categories.

The three laser intensity features expressing the largest difference between species were suggested as candidate features in our study. These were the maximum intensity (IMAX), mean intensity (IMEAN) of FIRST echoes, and the mean intensity (IMEAN) of LAST echoes. Mean intensity and standard deviation of intensity computed for all echoes were among the three best features in a Swedish study (Holmgren & Persson, 2004). In another Swedish study, mean intensity was incorporated as the third classification feature (Holmgren et al., 2008). However, Moffiet et al. (2005) found that raw intensity features did not contribute to species classification in their study. In a study in North America, three of the six best features were derived from the intensity distribution of first echoes (Brandtberg et al., 2003). Reitberger et al. (2008) found mean intensity of the tree useful in classification of coniferous and deciduous trees — both as a single feature and in combination with one or two other features.

4.6. Classification performance

In spite of the complex forest in the current study, the obtained classification accuracy of 88% for Large Trees is promising. In the current study, the sample trees were not segmented, but delineated on the basis of field measurements. Segmentation will most likely reduce the number of detected sub-dominant trees (Solberg et al., 2006) compared to the number of trees of these categories that were included in the current study. Thus, an increased classification accuracy would be expected if the trees were detected by a segmentation algorithm since less trees are detected and since these trees on average will have more laser echoes than the sub-dominant trees of this study. In other studies dealing with discrimination between coniferous and deciduous trees overall accuracies are at the same level as found in our study. Reitberger et al. (2008) obtain an overall accuracy of 85% classifying deciduous and coniferous trees whereas Holmgren et al. (2008) obtained an overall accuracy of 88% when classifying spruce, pine, and birch. Under leaf-off conditions Liang et al. (2007) achieve an overall accuracy of 90% when separating coniferous (spruce and pine) and deciduous (birch) trees. In another study conducted in the Østmarka forest reserve in which only intensity features were considered, an accuracy of 74% was achieved when classifying into three different categories, i.e., spruce, birch, and aspen trees (Ørka et al., 2007).

The overall classification accuracy for Small Trees was low (65%). Hence, classification of small individual trees may be a challenging task. The number of trees in the Small Trees category found by an segmentation algorithm will be low, since these trees likely are sub-dominant or suppressed (Solberg et al., 2006). In forest inventory tree species distribution for Small Trees may be classified using an area-based approach as an alternative to the individual tree classification. An area-based approach will have a higher number of echoes available to compute features from the echo distributions. Therefore, features will be more stable and may be more suitable for separating coniferous and deciduous tree species.

In addition to being influenced by crown characteristics, echo distributions are also affected by the laser acquisition parameter settings or sensor specific settings like e.g. pulse repetition frequency, beam divergence, and flying altitude (Chasmer et al., 2006; Goodwin et al., 2006; Hopkinson, 2007; Næsset, 2004b; Næsset, 2009). Thus, the selection of suitable features for tree species classification may be influenced by the ALS sensors and acquisition parameters used.

To conclude, promising classification results for spruce and birch were obtained using identified candidate ALS-derived structural- and intensity features. These candidate features included intensity features and different structural features derived from different echo categories. The echo category (FIRST, SINGLE, or LAST) is important in whether the feature is selected as a candidate feature or not. Further research should include validation of the suggested candidate variables on independent datasets, testing features from subsequent echoes of the same pulse, and assessment of radiometrically calibrated intensities.

References

Axelsson, P. (1999). Processing of laser scanner data—Algorithms and applications. *ISPRS Journal of Photogrammetry and Remote Sensing*, *54*, 138–147.

Baltsavias, E. P. (1999). Airborne laser scanning: Basic relations and formulas. *ISPRS Journal of Photogrammetry and Remote Sensing*, *54*, 199–214.

Bollandsås, O. M., & Næsset, E. (2007). Estimating percentile-based diameter distributions in uneven-sized Norway spruce stands using airborne laser scanner data. *Scandinavian Journal of Forest Research*, *22*, 33–48.

Boyd, D. S., & Hill, R. A. (2007). Validation of airborne LIDAR intensity values from a forested landscape using HYMAP data: Preliminary analysis. *International Archives of Photogrammetry, Remote Sensing and Spatial Information Sciences*, *XXXVI* Part 3/W52.

Brandtberg, T. (2002). Individual tree-based species classification in high spatial resolution aerial images of forests using fuzzy sets. *Fuzzy Sets and Systems*, *132*, 371–387.

Brandtberg, T. (2007). Classifying individual tree species under leaf-off and leaf-on conditions using airborne LIDAR. *ISPRS Journal of Photogrammetry and Remote Sensing*, *61*, 325–340.

Brandtberg, T., Warner, T. A., Landenberger, R. E., & McGraw, J. B. (2003). Detection and analysis of individual leaf-off tree crowns in small footprint, high sampling density LIDAR data from the eastern deciduous forest in North America. *Remote Sensing of Environment*, *85*, 290–303.

Brennan, R., & Webster, T. L. (2006). Object-oriented land cover classification of LIDAR-derived surfaces. *Canadian Journal of Remote Sensing*, *32*, 162–172.

Carleer, A., & Wolff, E. (2004). Exploitation of very high resolution satellite data for tree species identification. *Photogrammetric Engineering and Remote Sensing*, *70*, 135–140.

Chasmer, L., Hopkinson, C., Smith, B., & Treitz, P. (2006). Examining the influence of changing laser pulse repetition frequencies on conifer forest canopy returns. *Photogrammetric Engineering and Remote Sensing*, *72*, 1359–1367.

Coops, N. C., Hilker, T., Wulder, M. A., St-Onge, B., Newnham, G., Siggins, A., et al. (2007). Estimating canopy structure of Douglas-fir forest stands from discrete-return LIDAR. *Trees-Structure and Function*, *21*, 295–310.

Farid, A., Goodrich, D. C., & Sorooshian, S. (2006a). Using airborne LIDAR to discern age classes of cottonwood trees in a riparian area. *Western Journal of Applied Forestry*, *21*, 149–158.

Farid, A., Rautenkranz, D., Goodrich, D. C., Marsh, S. E., & Sorooshian, S. (2006b). Riparian vegetation classification from airborne laser scanning data with an emphasis on cottonwood trees. *Canadian Journal of Remote Sensing*, *32*, 15–18.

Gaveau, D. L. A., & Hill, R. A. (2003). Quantifying canopy height underestimation by laser pulse penetration in small-footprint airborne laser scanning data. *Canadian Journal of Remote Sensing*, *29*, 650–657.

Goodwin, N. R., Coops, N. C., & Culvenor, D. S. (2006). Assessment of forest structure with airborne LIDAR and the effects of platform altitude. *Remote Sensing of Environment*, *103*, 140–152.

Heurich, M. (2006). Evaluierung und entwicklung von automatiserten erfassung von waldstructuren aus daten flugzuggetragener fernerkundungssenoren. *Forstkuche Forshungsberichte München*, *2002*, 329.

Hodgson, M. E., & Bresnahan, P. (2004). Accuracy of airborne LIDAR-derived elevation: Empirical assessment and error budget. *Photogrammetric Engineering and Remote Sensing*, *70*, 331–339.

Holmgren, J. (2004). Prediction of tree height, basal area and stem volume in forest stands using airborne laser scanning. *Scandinavian Journal of Forest Research*, *19*, 543–553.

Holmgren, J., & Persson, Å. (2004). Identifying species of individual trees using airborne laser scanner. *Remote Sensing of Environment*, *90*, 415–423.

Holmgren, J., Persson, A., & Soderman, U. (2008). Species identification of individual trees by combining high resolution LIDAR data with multi-spectral images. *International Journal of Remote Sensing*, *29*, 1537–1552.

Hopkinson, C. (2007). The influence of flying altitude, beam divergence, and pulse repetition frequency on laser pulse return intensity and canopy frequency distribution. *Canadian Journal of Remote Sensing*, *33*, 312–324.

Hyde, P., Dubayah, R., Walker, W., Blair, J. B., Hofton, M., & Hunsaker, C. (2006). Mapping forest structure for wildlife habitat analysis using multi-sensor (LIDAR, SAR/InSAR, ETM plus, Quickbird) synergy. *Remote Sensing of Environment*, *102*, 63–73.

Hyyppä, H., & Hyyppä, J. (1999). Comparing the accuracy of laser scanner with other optical remote sensing data sources for stand attributes retrieval. *Photogrammetric Journal of Finland*, *16*, 5–15.

Hyyppä, J., Kelle, O., Lehikoinen, M., & Inkinen, M. (2001). A segmentation-based method to retrieve stem volume estimates from 3-D tree height models produced by laser scanners. *IEEE Transactions on Geoscience and Remote Sensing*, *39*, 969–975.

Key, T., Warner, T. A., McGraw, J. B., & Fajvan, M. A. (2001). A comparison of multispectral and multitemporal information in high spatial resolution imagery for classification of individual tree species in a temperate hardwood forest. *Remote Sensing of Environment*, *75*, 100–112.

Kline, R. B. (2004). *Beyond significance testing: Reforming data analysis methods in behavioral research.* Washington, D.C.: American Psychological Association.

Kaasalainen, S., Ahokas, E., Hyyppa, J., & Suomalainen, J. (2005). Study of surface brightness from backscattered laser intensity: Calibration of laser data. *IEEE Geoscience and Remote Sensing Letters*, *2*, 255–259.

Kraus, K., & Pfeifer, N. (1998). Determination of terrain models in wooded areas with airborne laser scanner data. *ISPRS Journal of Photogrammetry and Remote Sensing*, *53*, 193–203.

Liang, X., Hyyppä, J., & Matikainen, L. (2007). Deciduous–coniferous tree classification using difference between first and last pulse laser signatures. *International Archives of Photogrammetry, Remote Sensing and Spatial Information Sciences*, *XXXVI*, 253–257 PART 3/W52.

Magnussen, S., & Boudewyn, P. (1998). Derivations of stand heights from airborne laser scanner data with canopy-based quantile estimators. *Canadian Journal of Forest Research-Revue Canadienne De Recherche Forestiere*, *28*, 1016–1031.

Moffiet, T., Mengersen, K., Witte, C., King, R., & Denham, R. (2005). Airborne laser scanning: Exploratory data analysis indicates potential variables for classification of individual trees or forest stands according to species. *ISPRS Journal of Photogrammetry and Remote Sensing*, *59*, 289–309.

Morsdorf, F., Meier, E., Kotz, B., Itten, K. I., Dobbertin, M., & Allgower, B. (2004). LIDAR-based geometric reconstruction of boreal type forest stands at single tree level for forest and wildland fire management. *Remote Sensing of Environment*, *92*, 353–362.

Næsset, E. (2001). Effects of differential single- and dual-frequency GPS and GLONASS observations on point accuracy under forest canopies. *Photogrammetric Engineering and Remote Sensing*, *67*, 1021–1026.
Næsset, E. (2002). Predicting forest stand characteristics with airborne scanning laser using a practical two-stage procedure and field data. *Remote Sensing of Environment*, *80*, 88–99.
Næsset, E. (2004a). Accuracy of forest inventory using airborne laser scanning: Evaluating the first Nordic full-scale operational project. *Scandinavian Journal of Forest Research*, *19*, 554–557.
Næsset, E. (2004b). Effects of different flying altitudes on biophysical stand properties estimated from canopy height and density measured with a small-footprint airborne scanning laser. *Remote Sensing of Environment*, *91*, 243–255.
Næsset, E. (2004c). Practical large-scale forest stand inventory using a small-footprint airborne scanning laser. *Scandinavian Journal of Forest Research*, *19*, 164–179.
Næsset, E. (2009). Effects of different sensors, flying altitudes, and pulse repetition frequencies on forest canopy metrics and biophysical stand properties derived from small-footprint airborne laser data. *Remote Sensing of Environment*, *113*, 148–159.
Næsset, E., & Bjerknes, K. O. (2001). Estimating tree heights and number of stems in young forest stands using airborne laser scanner data. *Remote Sensing of Environment*, *78*, 328–340.
Nilsson, M. (1996). Estimation of tree weights and stand volume using an airborne LIDAR system. *Remote Sensing of Environment*, *56*, 1–7.
Olofsson, K., Wallerman, J., Holmgren, J., & Olsson, H. (2006). Tree species discrimination using Z/I DMC imagery and template matching of single trees. *Scandinavian Journal of Forest Research*, *21*, 106–110.
Ørka, H. O., Næsset, E., & Bollandsås, O. M. (2007). Utilizing airborne laser intensity for tree species classification. *International Archives of Photogrammetry, Remote Sensing and Spatial Information Sciences*, *XXXVI*, 300–304 Part 3/W52.
Persson, Å., Holmgren, J., & Söderman, U. (2002). Detecting and measuring individual trees using an airborne laser scanner. *Photogrammetric Engineering and Remote Sensing*, *68*, 925–932.
R Development Core Team (2007). *R: A language and environment for statistical computing.* Vienna: R Foundation for Statistical Computing.
Reitberger, J., Krzystek, P., & Stilla, U. (2008). Analysis of full waveform LIDAR data for the classification of deciduous and coniferous trees. *International Journal of Remote Sensing*, *29*, 1407–1431.
Reutebuch, S. E., McGaughey, R. J., Andersen, H. E., & Carson, W. W. (2003). Accuracy of a high-resolution LIDAR terrain model under a conifer forest canopy. *Canadian Journal of Remote Sensing*, *29*, 527–535.
Schreier, H., Lougheed, J., Tucker, C., & Leckie, D. (1985). Automated measurements of terrain reflection and height variations using an airborne infrared laser system. *International Journal of Remote Sensing*, *6*, 101–113.
Silverman, B. W. (1986). *Density estimation.* London: Chapman and Hall.
Solberg, S., Næsset, E., & Bollandsås, O. M. (2006). Single tree segmentation using airborne laser scanner data in a structurally heterogeneous spruce forest. *Photogrammetric Engineering and Remote Sensing*, *72*, 1369–1378.
Song, J., Han, S., Yu, K., & Kim, Y. (2002). Assessing the possibility of land-cover classification using LIDAR intensity data.*International Archives of Photogrammetry, Remote Sensing and Spatial Information Sciences*, *XXXIV*, 256–259 Part 3B.
Terrasolid Ltd. (2004). *TerraScan user's guide.* Helsinki: Terrasolid Ltd.
Venables, W. N., & Ripley, B. D. (2002). *Modern applied statistics with S.* New York: Springer.
Wehr, A., & Lohr, U. (1999). Airborne laser scanning — An introduction and overview. *ISPRS Journal of Photogrammetry and Remote Sensing*, *54*, 68–82.
Wotruba, L., Morsdorf, F., Meier, E., & Nüesch, D. (2005). Assessment of sensor characteristics of an airborne laser scanner using geometric reference targets. *International Archives of Photogrammetry, Remote Sensing and Spatial Information Sciences*, *XXXVI*, 1–7 Part 3/W19.